Bugoi *et al. Herit Sci* (2019) 7:55
https://doi.org/10.1186/s40494-019-0298-2

Heritage Science

RESEARCH ARTICLE Open Access

Archaeometric characterization of Byzantine pottery from *Păcuiul lui Soare*

Roxana Bugoi[1*], Cristina Talmaţchi[2], Constantin Haită[3] and Daniele Ceccato[4,5]

Abstract

Archaeometric investigations using OM (optical microscopy) and micro-PIXE (particle induced X-ray emission) were performed on 45 ceramic shards unearthed in archaeological excavations at *Păcuiul lui Soare* (southeastern Romania) and dated to the eleventh century AD. This study aimed to get clues about the raw materials and manufacturing techniques used by the potters from the Lower Danube area during the Byzantine period. The analyzed ceramic fragments were selected according to stylistic and archaeological criteria, trying to cover the entire palette of potteries discovered at this site. OM detailed the characteristics of the fabric (texture, microstructure and porosity), mineralogy, surface treatments and firing of the shards. Principal component analysis (PCA) of the PIXE data highlighted two main categories of shards with distinct compositional signatures, separated mainly by their aluminum and calcium content. Micro-PIXE maps of the interfaces between the glaze and the ceramic body showed that the green glaze is rich in lead oxide compared to the underlying ceramic body. The results of these investigations were compared to the ones previously obtained on coeval potteries from other Byzantine archaeological sites, i.e. *Hârşova* and *Oltina*, trying to get some hints about the consumption and circulation of pottery in the Lower Danube region at the beginning of the second millennium AD.

Keywords: Byzantine, Ceramic, *Păcuiul lui Soare*, Micro-PIXE, Optical microscopy, Lead glaze

Introduction

Archaeometric investigations of Byzantine ceramics are relatively scant, only the recent years witnessing an increase in the number of the publications on this topic [1–6 and references therein]. This statement also applies for the Byzantine pottery excavated on nowadays Romania's territory [7–9].

Until now, the studies dedicated to the ceramic trade in Dobrudja were exclusively based on stylistic analogies between similar finds discovered at different sites [10–13]; however, these publications do not contain any analytical data.

This research was conducted on an assemblage of 45 ceramic shards excavated at the fortress from *Păcuiul lui Soare* (see Fig. 1) located on the eponymous island on the Danube river (see Fig. 2). The shards were found in secure archaeological contexts; all of them were dated to the eleventh century AD according to stratigraphic and typological criteria. The selected fragments can be considered as representative for all the ceramic finds discovered until now at this archaeological site.

Through this study, we try to answer the following questions: Are there any potteries different from the ones positively identified as local products on archaeological grounds? Can we identify the ceramic vessels supposedly imported to *Păcuiul lui Soare* based on mineralogical and chemical criteria Can we get any information about the techniques and resources employed to manufacture these utilitarian products?

To reach these goals, OM was used to describe the fabric and the mineralogy of the selected ceramic fragments, while PIXE provided the compositional characterization of the shards. The analytical information was used to get some hints about the raw materials and manufacturing techniques, trying to verify if the stylistic and typological differences between the shards are also reflected by distinctive morphological and physico-chemical features.

*Correspondence: bugoi@nipne.ro
[1] Horia Hulubei National Institute for Nuclear Physics and Engineering, 30 Reactorului Street, 077125 Măgurele, Romania
Full list of author information is available at the end of the article

Fig. 1 Map showing the location of *Păcuiul lui Soare*, the archaeological site where the shards analyzed in this study were excavated. For comparison, *Hârşova* and *Oltina* are also indicated

This study is a stage of an ongoing archaeometric project targeting the systematic multidisciplinary characterization of Byzantine ceramic dated to the eighth to twelfth centuries AD excavated in Dobrudja, the historical province located in the south-eastern part of Romania between Danube and the Black Sea—see Fig. 1. Based on this information, this project attempts to produce analytical evidences for the commercial exchanges between the centers from the Lower Danube region during the Byzantine ruling.

Historical and archaeological background

The fortress from *Păcuiul lui Soare* was raised by the Byzantines during the second half of the tenth century AD. Established as a naval basis [14], the fortress played an important role in controlling the navigation on the Danube and protecting Dorostolon, the capital of the Byzantine Theme Dristra/Paradunavon—nowadays Silistra. During the eleventh century AD, *Păcuiul lui Soare* lost its military importance and turned into a civilian settlement [15]. In 1094, a Cuman attack practically stopped the habitation of the site for more than 100 years [16].

Păcuiul lui Soare was situated on a well-known commercial route of the epoch, namely the Danube river, that connects Central Europe with the Black Sea and the Middle East. This special location made *Păcuiul lui Soare* a powerful commercial center during the eleventh century AD. Commodities from Europe, Central Asia and Middle East arrived at this point, as demonstrated by the impressive archaeological discoveries and by the existence of a harbor from which only a 42 m long quay survived until today [16].

The ceramic material analyzed in this study comes from sealed contexts, as well as from the occupation layer. The analyzed shards were dated between 1001 and 1094 AD.

There are strong archaeological evidences indicating that ceramic vessels were produced at *Păcuiul lui Soare* during the first half of the eleventh century AD. Thus, during the 1973 excavation campaign, a pottery kiln was discovered inside the fortress, close to the northern gate [17]—see Fig. 2. Inside this kiln, some ceramic vessels in fragmentary state and some refuses were found, suggesting that pots and cauldrons were produced here. In the filling of the access pit of the kiln, several amphorae fragments were also discovered. The finding of the amphorae shards nearby the kiln, as well as the discovery in 1971 of a bronze stamp for marking amphorae suggest the production of this type of potteries at *Păcuiul lui Soare* alongside with other types of vessels [18].

Materials and methods

Materials

To answer the above-mentioned questions, a set of 45 ceramic shards excavated at *Păcuiul lui Soare* were selected for this archaeometric study; they are considered representative for all potteries discovered until now at this site. The ceramic fragments derived from different types of vessels, being either manufactured from common clay or from "kaolinitic" clays, with fine or coarse paste, covered with olive-green glaze, golden engobe or with incised decorations, painted or not, originating from cooking or storage vessels, etc. In particular, the studied shards are fragments of cauldrons, jugs, pots with or without handles, bowls, amphorae, and rush lights. For a more detailed description of the ceramic samples under scrutiny, the reader is referred to Table 1 and Fig. 3.

Glazed shards represent 5% of the overall ceramics finds excavated until now at *Păcuiul lui Soare*. The glaze is olive-green, with hues varying from light to dark olive-green, sometimes with reddish reflections. The glaze is matte or shiny, being either uniformly or unevenly applied, mostly on the outer surface of the vessels. In most cases, the glaze was well preserved. Shard P2 from Fig. 3 is covered with a shining glaze without any exfoliation. However, the glaze is lacking from several small zones of this shard. This partial absence of the external decoration is not an effect of the burial, but it can be explained by the fact that the glaze was not uniformly applied on the entire surface of the vessel, suggesting a less careful manufacturing process.

An important category of ceramic finds from *Păcuiul lui Soare* is the one of potteries made of "whitish clays" [14], a term cautiously used to describe the shards presenting the visual characteristics of kaolinitic paste, i.e.

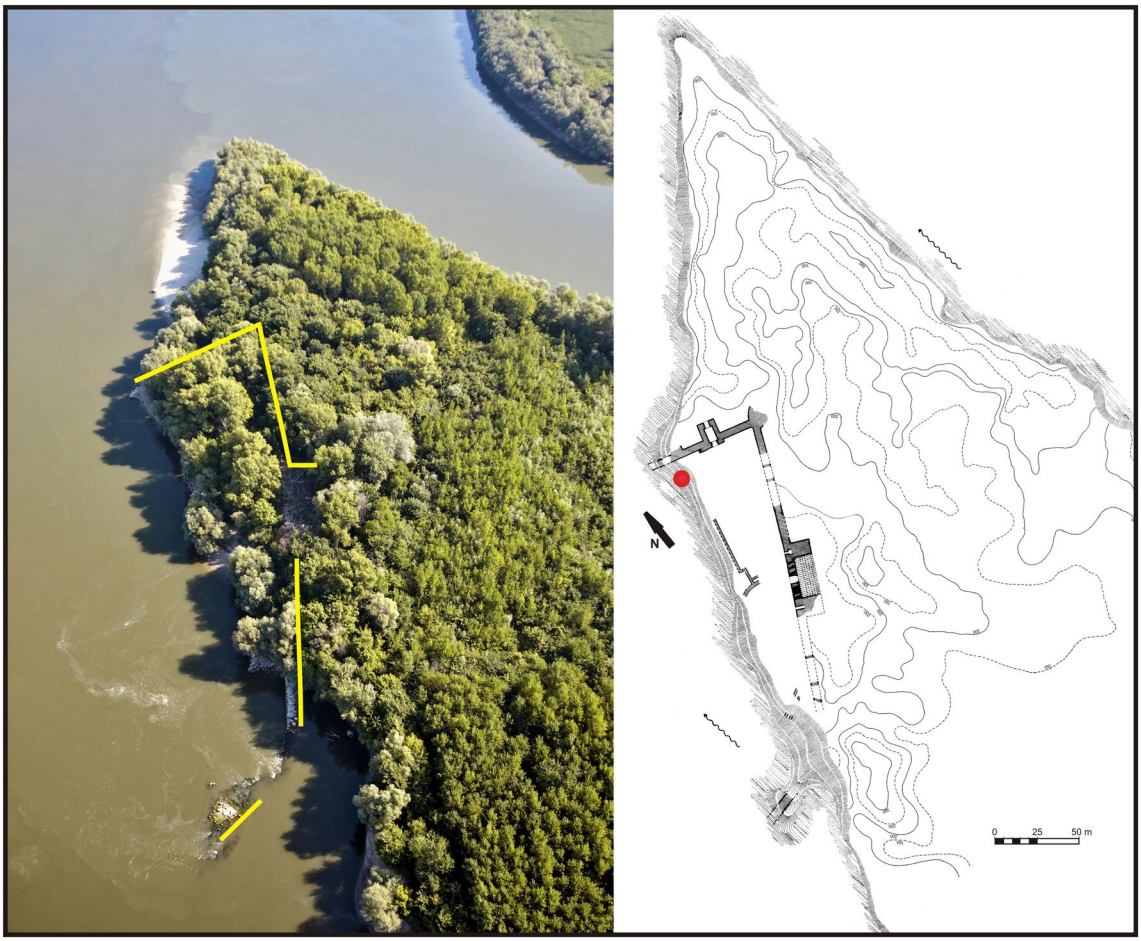

Fig. 2 Left side—aerial view of the north-eastern part of *Păcuiul lui Soare* island, on which the part of the fortress still existing today is evidenced (Photo credits: Mircea Stoian); Right side—layout of the surviving *Păcuiul lui Soare* fortress (after [14], Fig. 3) on which the finding place of the ceramic kiln is marked with a red dot

light grey, yellow, pale yellow with pinkish white and pink hues and reddish rounded inclusions [19].

Due to the fact that they were rare occurrences among the ceramic finds from *Păcuiul lui Soare*, it was presumed that the glazed shards and the ones with golden engobe represent imported potteries.

Methods

Optical microscopy

In order to characterize the ceramic paste, the 45 ceramic samples were initially studied with a stereomicroscope with magnifications of $\times 10...\times 30$. This preliminary investigation showed that all the shards can be classified into four types of ceramic paste. Subsequently, 15 shards were selected to prepare thin sections that can be considered representative for the entire batch of 45 ceramic fragments. To detail the types of paste and to perform the mineralogical characterization, the thin sections were analyzed using an Olympus BX 60 polarizing petrographic microscope at magnifications varying from $\times 50$ to $\times 500$. The microscopic description was made following the guidelines of thin section analysis [20–22], based on the textural characteristics (granulometry, sorting, frequency and grain shapes), composition (nature of mineral and organic constituents), microstructure, porosity, firing and surface treatment [21].

PIXE

PIXE measurements were performed on samples extracted from all shards at AN2000 accelerator of LNL, INFN, Italy, with a 2 MeV proton beam [23], using macro-beam settings (beam size $\sim 3 \times 3$ mm^2) and a preset charge of 4 μC. The IGLET-X™ HPGe detector from ORTEC® used for X-rays detection was covered

Table 1 Archaeological description of the ceramic samples analyzed in this study

Sample ID	Type of clay (archaeological criteria)	Vessel	External surface decoration	OM type	PCA group
P1	Common clay	Jug	Olive-green glaze	III	II
P2	Common clay	Jug	Olive-green glaze	III	II
P3	Common clay	Jug	Olive-green glaze	III	II
P4	Common clay	Jug	Olive-green glaze	III	II
P5	Common clay	Jug	Olive-green glaze	II	II
P6	Common clay	Cup	Olive-green glaze	III	II
P7	Common clay	Jug	Olive-green glaze	III	II
P8	Common clay	Jug	Golden micaceous engobe	II	II
P9	Common clay	Jug	Golden micaceous engobe	II	II
P10	Common clay	Jug	Golden micaceous engobe	II	II
P11	Common clay	Jug	Golden micaceous engobe	II	II
P12	Common clay	Spheroidal amphora	Bright yellow engobe	II	II
P13	Common clay	Spheroidal amphora	Yellow cream engobe	II	II
P14	Common clay	Spheroidal amphora		II	I
P15	Kaolinitic clay	Bowl	Red paint lines	I	I
P16	Kaolinitic clay	Bowl		I	I
P17	Kaolinitic clay	Bowl		I	I
P18	Kaolinitic clay	Pot		I	I
P19	Kaolinitic clay	Pot		I	I
P20	Kaolinitic clay	Pot		I	I
P21	Kaolinitic clay	Bowl		I	I
P22	Kaolinitic clay	Cauldron		I	I
P23	Kaolinitic clay	Pot		I	I
P24	Kaolinitic clay	Pot		I	I
P25	Kaolinitic clay	Pot		I	I
P26	Kaolinitic clay	Pot		I	I
P27	Kaolinitic clay	Pot		I	I
P28	Kaolinitic clay	Pot		I	I
P29	Kaolinitic clay	Pot		I	I
P30	Kaolinitic clay	Pot		I	I
P31	Common clay	Jug		II	II
P32	Common clay	Cauldron		II	II
P33	Common clay	Cauldron		IV	II
P34	Common clay	Rush-light		IV	II
P35	Common clay	Pot?		IV	II
P36	Common clay	Pot?		III	II
P37	Common clay	Pot		IV	II
P38	Common clay	Pot		IV	I
P39	Common clay	Pot		III	II
P40	Common clay	Pot		IV	II
P41	Common clay	Pot		II	II
P42	Kaolinitic clay	Pot		I	II
P43	Common clay	Pot?		II	II
P44	Common clay	Storage vessel		II	II
P45	Common clay	Storage vessel		II	II

The paste types resulting from OM, as well as the compositional categories resulting from PCA of the PIXE data are also in indicated in the last two columns

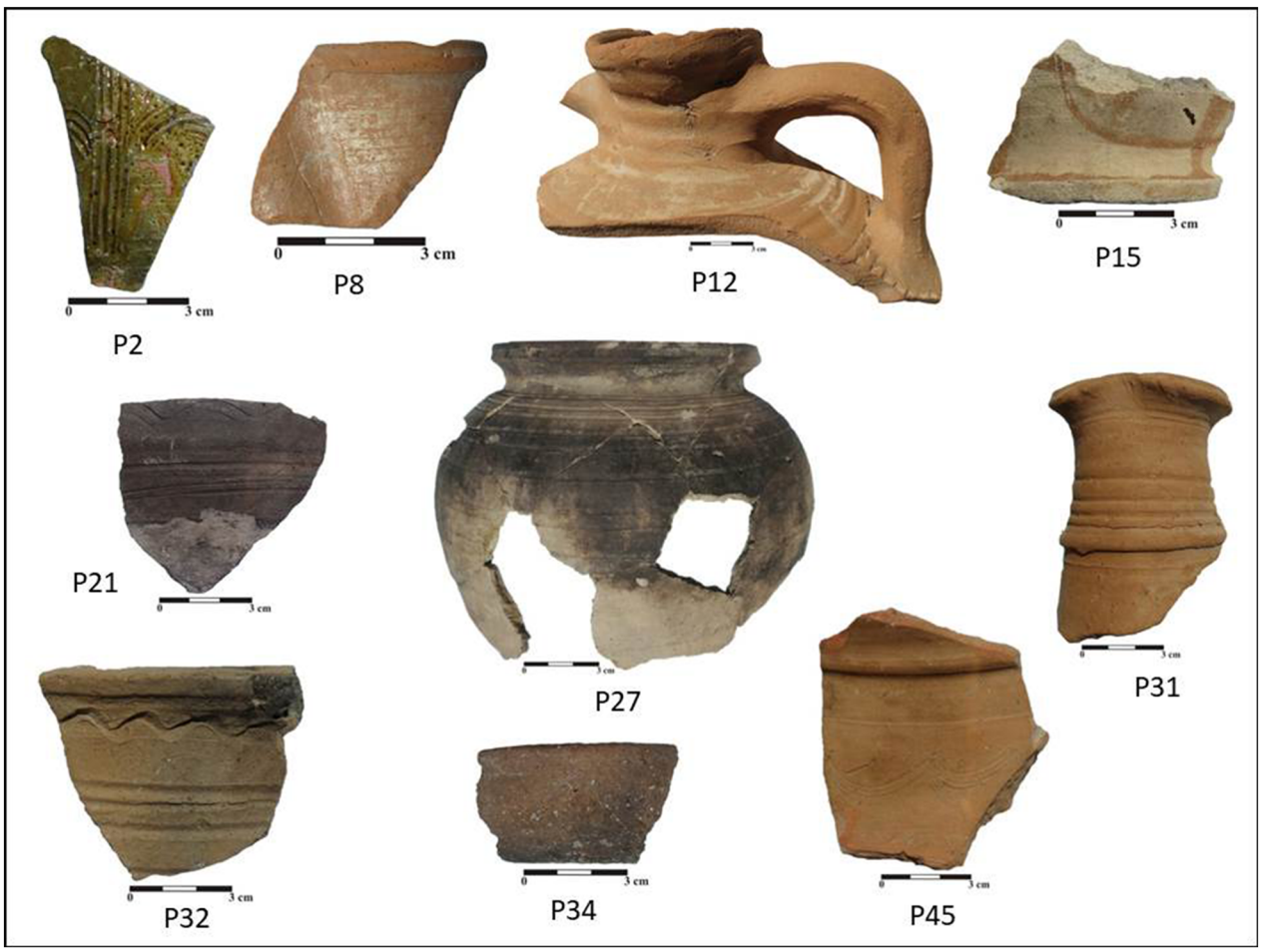

Fig. 3 Photos of some ceramic finds from *Păcuiul lui Soare*

with a 100 μm thick Al funny filter (0.7%) that enabled the reduction of the intense peaks of low-Z elements in the characteristic X-ray spectra. An example of a PIXE spectrum is given in Fig. 4.

Using an agate mortar, small ceramic fragments broken from each shard were transformed into powders that were subsequently pelletized. The interfaces between the glaze layers and the underlying ceramic bodies were measured with the micro-beam (beam size $\sim 4 \times 4$ μm^2), by scanning 750×750 μm^2 areas on the shards as such. To obtain the glaze composition, small zones on the decorated surface of shards were bombarded with the proton beam without any preparation.

To obtain quantitative results, PIXE spectra were treated with GUPIXWIN software (version 2.2.4) [24], considering all the detected elements (Mg, Al, Si, P, S, Cl, K, Ca, Ti, Cr, Mn, Fe, Ni, Cu, Zn, Ga, Rb, Sr, Y, Zr, Pb, Sb) as oxides (except for Cl), and normalizing the concentrations to 100 mass%.

Basalt BHVO-2 Certified Reference Material (CRM) was used to assess the accuracy of the quantitative results. The overall uncertainties were estimated to around 5% for the major elements, varying from 10% up to 30% for the minor elements and trace-elements.

The detection limits of the employed experimental set-up for a ceramic target are given in Table 2, while the results of the PIXE analyses—chemical composition of the ceramic body and green glaze—are presented in Tables 3 and 4, respectively.

Results and discussion

Results

Optical microscopy

Using OM, four main types of ceramic paste were identified for the *Păcuiul lui Soare* shards. Their description is given in the lines below; their assignation to a certain type of paste is summarized in Table 1.

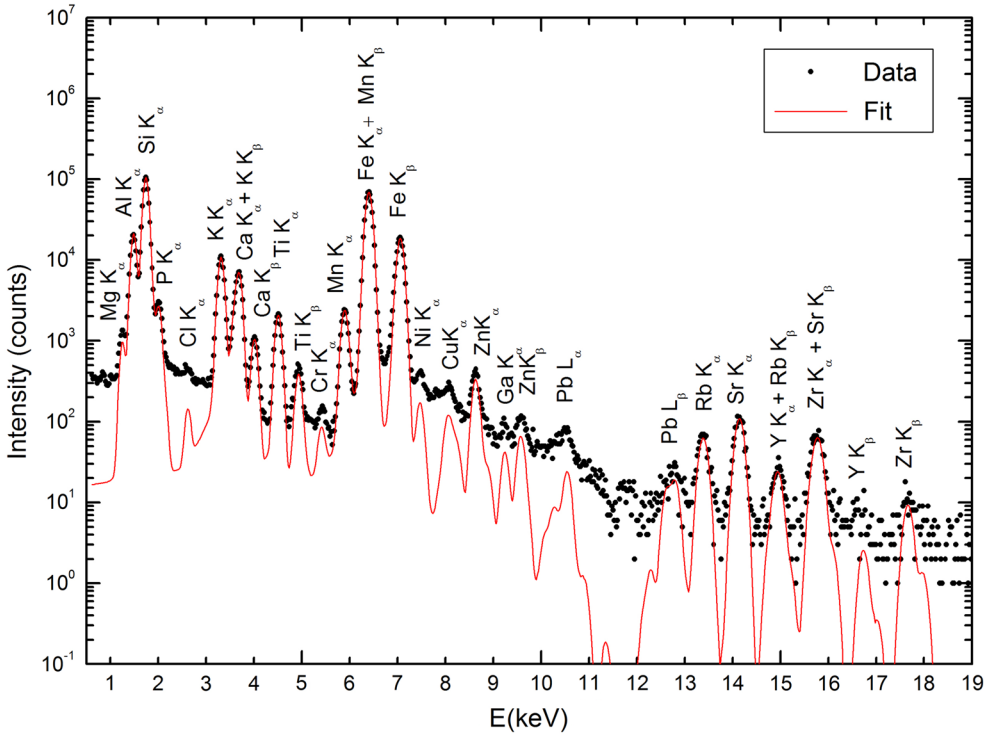

Fig. 4 PIXE spectrum of sample P31

Table 2 Detection limits (expressed in ppm) of the employed experimental set-up for a ceramic matrix

Oxide/element	DL (ppm)
MgO	740
Al_2O_3	435
SiO_2	250
P_2O_5	550
SO_3	445
Cl	77
K_2O	50
CaO	190
TiO_2	55
Cr_2O_3	40
MnO	30
Fe_2O_3	65
NiO	15
CuO	13
ZnO	7
Ga_2O_3	7
Rb_2O	11
SrO	7
Y_2O_3	17
ZrO_2	28
PbO	25

I. Fine paste with silty clay matrix, oriented microstructure and micro-fissures: P15, P16, P17, P18, P19, P20, P21, P22, P23, P24, P25, P26, P27, P28, P29, P30, P42.

Fine, homogeneous paste with fine silty clay matrix with rare (5–10%) silt grains, 10–50 μm, and more frequent (10–15%) fine sand grains, 100–250 μm, rarely medium sand, 300–500 μm, and accidental coarse grains, 1.0–1.4 mm; mono- and polycrystalline (for coarse sand fraction) quartz and feldspar, frequent amorphous ferruginous stains and concretions, 10–30 μm, and rarely (1–2%) much larger, i.e. 100–300 μm. Low porosity (5–15%), with fine isolated pores, 100–300 μm, and more frequent micro-fissures, 0.5–3.0 mm. The clay is birefringent, the sand grains are sub-rounded and rounded, being intentionally added to the silty clay matrix. This paste shows a good to moderate sorting; mica flakes are absent (Fig. 5a). These vessels were fired in oxidizing conditions, complete or incomplete ("banded" structure). In some cases, secondary firing is present, as some of these shards were fragments of cooking pots or because some fragments were discovered in burned dwellings.

Table 3 Chemical composition data determined by PIXE for ceramic body expressed in mass% for major and minor elements and ppm for traces ("0" means below the detection limits)

	MgO (mass%)	Al_2O_3 (mass%)	SiO_2 (mass%)	P_2O_5 (mass%)	SO_3 (ppm)	Cl (ppm)	K_2O (mass%)	CaO (mass%)	TiO_2 (mass%)	Cr_2O (ppm)	MnO (ppm)
P1	2.7	18.4	66.3	0	0	0	2.5	2.5	0.9	0	919
P2	2.0	18.3	67.9	0.4	0	0	3.1	1.3	1.0	216	910
P3	2.7	17.1	63.7	0.9	922	0	2.9	5.7	0.9	224	1277
P4	2.0	16.8	70.9	0.4	0	0	2.4	1.4	0.9	165	864
P5	2.4	17.5	69.4	0.0	0	0	2.9	1.3	1.0	454	912
P6	2.2	17.3	67.5	0.5	1556	0	2.8	2.6	1.0	168	640
P7	2.6	18.2	65.4	0.4	0	0	3.1	3.3	0.9	158	980
P8	3.6	19.8	58.0	0.4	521	189	3.4	6.3	1.0	274	1335
P9	2.6	17.1	63.3	0.6	0	0	2.9	6.8	1.0	160	941
P10	1.9	16.2	63.7	0.7	2506	571	2.8	8.7	0.9	215	725
P11	3.2	17.6	60.8	1.0	837	1276	3.1	6.9	1.1	160	1074
P12	4.9	18.1	57.2	0.4	0	0	3.2	7.9	1.0	463	1026
P13	4.3	18.2	58.1	0.5	0	283	3.7	7.0	1.0	399	1158
P14	1.1	23.2	69.8	0.5	0	395	1.3	0.8	1.1	124	337
P15	0.9	25.0	68.3	0.1	0	0	2.2	0.5	1.0	118	122
P16	1.2	23.5	69.6	0.4	0	505	1.3	0.7	1.1	85	351
P17	1.2	22.5	71.2	0.1	0	176	1.4	0.6	1.1	93	180
P18	1.3	26.0	62.0	0.2	0	179	1.6	1.7	1.3	204	141
P19	1.1	26.6	65.7	0.5	697	702	1.4	1.2	1.1	153	84
P20	0.9	28.6	59.2	0.6	885	226	1.3	0.8	1.3	217	326
P21	1.2	22.9	63.0	0.5	0	746	1.7	1.0	1.7	266	225
P22	1.0	24.0	67.3	0.3	0	217	1.3	1.1	1.2	146	327
P23	1.1	24.6	67.3	0.6	867	927	1.2	1.3	1.2	118	206
P24	1.3	22.7	69.4	0.2	0	0	1.4	0.6	1.4	149	252
P25	1.1	28.6	55.7	0.4	727	270	1.3	1.1	1.3	225	627
P26	1.0	26.7	61.9	0.9	684	0	1.7	1.2	1.3	163	318
P27	1.3	21.3	68.5	0.1	0	106	1.8	0.5	1.2	122	120
P28	1.3	26.2	64.2	0.3	0	0	1.3	0.6	1.3	184	304
P29	1.1	27.4	60.3	0.5	1088	308	1.0	1.2	1.3	241	180
P30	1.1	24.5	65.1	0.6	0	202	1.3	1.6	1.2	176	255
P31	1.9	17.3	63.4	2.5	0	320	3.0	2.3	1.1	166	3742
P32	2.9	17.9	64.2	0.5	935	244	3.2	3.3	0.9	311	637
P33	2.7	15.0	70.2	0.5	0	179	2.5	2.8	0.8	183	1057
P34	3.1	17.2	61.9	0.3	784	266	4.6	3.7	0.6	224	339
P35	3.2	17.4	63.8	0.2	593	209	4.5	0.8	0.7	208	524

Table 3 (continued)

	MgO (mass%)	Al_2O_3 (mass%)	SiO_2 (mass%)	P_2O_5 (mass%)	SO_3 (ppm)	Cl (ppm)	K_2O (mass%)	CaO (mass%)	TiO_2 (mass%)	Cr_2O (ppm)	MnO (ppm)
P36	2.2	16.8	60.6	0.7	2739	610	5.8	5.5	0.9	237	1145
P37	2.5	17.1	63.8	1.3	0	0	2.9	4.6	0.9	229	1353
P38	1.6	24.7	65.0	0.7	1196	292	1.1	1.2	1.0	201	0
P39	2.5	16.9	63.8	1.0	0	248	3.1	4.9	1.0	208	1125
P40	6.2	19.7	58.7	1.0	1291	444	2.7	4.2	0.8	239	1702
P41	2.9	18.6	59.7	0.9	0	0	3.1	3.9	1.0	152	888
P42	3.8	18.8	62.7	0.6	0	381	2.7	3.9	0.8	291	415
P43	5.3	17.1	59.5	0.6	1206	835	3.9	3.2	0.6	246	0
P44	3.7	19.3	61.9	0.5	1481	2754	3.5	1.5	1.0	234	993
P45	1.9	17.3	65.4	0.6	810	234	3.3	1.7	1.1	232	1342

	Fe_2O_3 (mass%)	NiO (ppm)	CuO (ppm)	ZnO (ppm)	Ga_2O_3 (ppm)	Rb_2O (ppm)	SrO (ppm)	Y_2O_3 (ppm)	ZrO_2 (ppm)	PbO (ppm)
P1	5.6	91	0	109	0	0	164	0	0	2645
P2	5.7	59	25	106	27	147	110	0	314	249
P3	5.5	89	49	164	32	103	173	0	400	1628
P4	4.8	59	0	93	0	90	109	57	307	1102
P5	5.2	59	33	112	24	124	125	0	243	55
P6	5.2	78	43	100	0	113	156	0	180	3918
P7	5.7	61	46	132	23	144	148	0	456	484
P8	7.1	152	47	220	23	160	179	39	171	107
P9	5.3	67	29	136	21	124	209	0	300	0
P10	4.5	67	38	106	17	84	341	58	276	0
P11	5.9	110	34	179	26	153	268	0	195	86
P12	7.1	254	58	146	31	121	214	0	141	54
P13	7.0	216	64	144	28	135	180	0	168	31
P14	1.9	18	13	53	26	57	57	0	269	27
P15	2.0	20	0	39	31	73	51	36	276	27
P16	1.9	12	13	47	26	69	86	29	271	21
P17	1.8	19	14	35	32	62	47	37	279	43
P18	5.7	26	0	57	33	84	111	0	317	33
P19	2.3	21	16	36	29	40	69	50	469	40
P20	7.1	35	23	73	45	37	154	0	313	51
P21	7.8	39	36	115	53	105	118	0	576	0
P22	3.4	23	21	65	49	80	97	34	584	50

Table 3 (continued)

	Fe_2O_3 (mass%)	NiO (ppm)	CuO (ppm)	ZnO (ppm)	Ga_2O_3 (ppm)	Rb_2O (ppm)	SrO (ppm)	Y_2O_3 (ppm)	ZrO_2 (ppm)	PbO (ppm)
P23	2.3	28	0	58	32	61	101	25	357	35
P24	2.8	36	29	65	47	100	106	62	470	36
P25	10.3	41	26	119	54	55	193	36	420	38
P26	5.1	42	28	96	40	68	157	36	354	54
P27	5.1	33	31	77	45	124	69	58	383	40
P28	4.5	0	17	75	45	82	196	0	452	51
P29	7.0	37	26	80	42	59	166	28	437	30
P30	4.4	37	26	60	34	65	172	27	455	42
P31	8.0	110	60	209	30	121	312	53	260	58
P32	6.7	100	52	166	28	174	244	53	330	90
P33	5.3	57	39	142	23	124	202	36	342	36
P34	8.4	74	35	172	33	199	144	0	102	50
P35	9.1	89	47	192	32	238	139	0	94	55
P36	6.9	87	82	250	29	237	229	45	492	59
P37	6.5	84	64	182	24	154	363	35	354	106
P38	4.5	0	72	61	55	63	100	56	401	49
P39	6.4	88	54	168	29	138	304	46	454	63
P40	6.3	58	86	200	46	177	203	29	217	96
P41	9.5	166	75	251	31	232	356	0	257	101
P42	6.2	78	92	200	57	178	200	45	350	104
P43	9.2	58	71	201	59	287	191	0	121	0
P44	7.8	42	91	201	40	189	201	53	1713	180
P45	8.3	107	57	488	37	200	195	85	544	160

Results were normalized to 100%; "0" values in the table means below the detection limits—see Table 2

Table 4 Chemical composition data determined by PIXE for the green glaze expressed in mass% for major and minor elements and ppm for traces ("0" means below the detection limits)

	MgO (mass%)	Al_2O_3 (mass%)	SiO_2 (mass%)	K_2O (mass%)	CaO (mass%)	TiO_2 (mass%)	MnO (ppm)	Fe_2O_3 (mass%)	NiO (ppm)	CuO (ppm)	ZnO (ppm)	Sb_2O_5 (mass%)	PbO (mass%)
P1	1.4	5.7	20.4	0.5	1.9	0.3	456	2.5	1847	596	140	1.3	65.4
P2	1.1	3.6	12.5	0.5	0.9	0.3	451	3.2	2228	1351	162	0.6	75.7
P3	2.2	4.8	20.3	0.6	3.4	0.2	633	2.2	1894	1127	506	0	65.4
P4	0.8	4.8	23.0	1.2	2.1	0.4	0	2.1	1855	537	123	0	65.3
P5	1.6	5.5	25.3	1.3	12.8	0.3	0	1.9	1548	443	190	0	50.4
P6	0.7	4.4	24.0	1.5	1.1	0.2	0	1.7	1974	759	0	0	65.9
P7	1.1	6.5	24.8	1.2	2.3	0.3	238	2.5	1745	4059	87	0	60.6

Results were normalized to 100%; "0" values in the table means below the detection limits—see Table 2

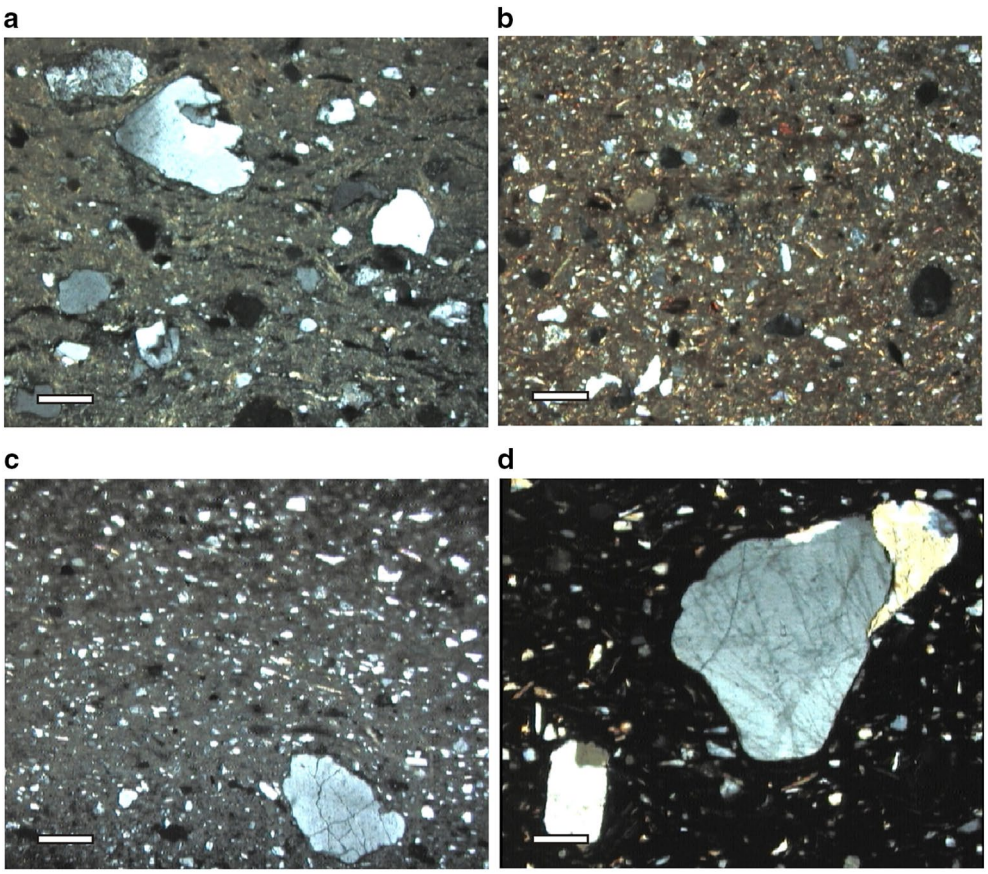

Fig. 5 OM micrographs of thin sections considered as representative for the main paste types. All images are in cross polarized light. **a** Fine silty clay oriented paste, with medium sand grains of quartz and feldspar (scale bar: 200 μm). **b** Fine silty porphyritic paste, with fine sand grains and muscovite flakes (scale bar: 200 μm). **c** Fine carbonate porphyritic paste, with fine sand grains and muscovite flakes (scale bar: 200 μm). **d** Medium granular porphyritic paste, with fine muscovite flakes and medium to coarse sand grains (scale bar: 200 μm)

II. Fine silty paste with porphyritic microstructure: P5, P8, P9, P10, P11, P12, P13, P14, P31, P32, P41, P43, P44, P45.
Fine, homogeneous paste with fine grained silty matrix, well sorted, with frequent (15–25%) grains of fine sand; mono- and polycrystalline quartz and feldspar, 50–100 μm, rarely 150–200 μm and frequent mica (predominant muscovite), 50–200 μm, frequent fine vegetal debris, 20–150 μm, ferruginous stains and concretions, 50–150 μm, rare fine carbonate grains, 100–400 μm, and accidental shell fragments. Fine porosity (5–10%), with frequent isolated and rounded voids, 50–200 μm, very rarely up to 1 mm. Rare elongated voids originating from vegetal temper are present. This paste was most probably made from alluvial sediments, well sorted silt with fine sand and clay; sand grains are sub-rounded and rounded (Fig. 5b). These shards were fired in complete or incomplete (with dark organic "core") oxidizing conditions.

III. Fine carbonate paste with porphyritic microstructure: P1, P2, P3, P4, P6, P7, P36, P39.
Fine, homogeneous paste with fine carbonate matrix, with frequent (10–15%) fine silty grains, 10–50 μm, rare fine sand, 50–200 μm, and very rare (2–3%) medium to coarse sand grains, 400–750 μm; sand fraction with mono- and polycrystalline quartz and feldspars, rare (5%) fine flakes of mica, 50–150 μm, rare calcite grains, 100–200 μm and opaque grains, 50–100 μm (Fig. 5c). This paste includes areas of calcite recrystallization on voids and fine cracks. Low porosity (5–10%), with fine circular voids, 50–300 μm, and rare mm-size micro-fissures are visible. This paste was made from carbonated sediments (unconsolidated marl type), featuring a well-sorted matrix, with possible mixture of fine sand with medium to coarse sand grains, that are generally sub-rounded and rounded. The shards were fired in oxidizing conditions, featuring a banded structure and an organic "core".

IV. Medium granular paste with porphyritic microstructure: P33, P34, P35, P37, P38, P40.
Semi-fine, homogeneous paste, with silty clay with fine sand matrix, moderately to poorly sorted; rare silty grains (5%), 20–50 μm, and frequent very fine sand (10–20%), 50–200 μm. It includes rare coarse sand grains (1–5%), 500–1500 μm. This paste is similar with the fine silty paste (type II), with frequent fine mica flakes, 50–200 μm, but with frequent quartz and quartzite sand inclusions, with heterogeneous appearance (Fig. 5d). Fine porosity, 10–15%, isolated voids, 50–200 μm, circular and elongated, irregular, and micro-fissures, 100–300 μm, rarely 0.5–1.5 mm. The sand grains are sub-angular, sub-rounded and rounded. These shards were fired in reducing conditions, with an organic "core", being oxidized at the exterior.

The four main types of ceramic paste identified for the ceramic fragments from *Păcuiul lui Soare* are similar to the ones evidenced for the coeval potteries discovered in the nearby archaeological sites *Hârșova* and *Oltina* that were previously analysed in the frame of the on-going project mentioned in "Introduction" section [7, 8].

The fine paste with silty clay matrix (type I) is made from a mixture of sediments, silty clay and fine sand, with oriented and birefringent clay, possibly kaolinitic, such as the one identified in the two aforementioned sites.

The silty paste with porphyritic structure (type II) is made of fine alluvial sediments. As in the other two archaeological sites studied until now (*Hârșova* and *Oltina*) this is indicated by the good sorting of the sedimentary matrix, the presence of the vegetal debris (partially decayed fragments of wood), and accidentally, of the shell fragments.

The fine carbonate paste (type III) is most probably made of fine alluvial sediments deposited in low energy sedimentary environments, such as marshy areas or lakes.

The medium granular paste (type IV) is made of silty fine sands with clay, very probably alluvial, mixed with coarse alluvial sands with variable granulometry.

PIXE

To get a clear picture about the possible grouping of the ceramic shards according to their composition, taking into account the relatively large number of samples and variables, PCA (Principal Components Analysis) of the standardized PIXE data—Mg, Al, K, Ca, Ti, Cr, Fe, Ni, Cu, Zn, Ga, Rb, Sr and Zr oxides—was performed using STATISTICA software (version 8.0). Figure 6 shows the result of this analysis indicating the separation of the

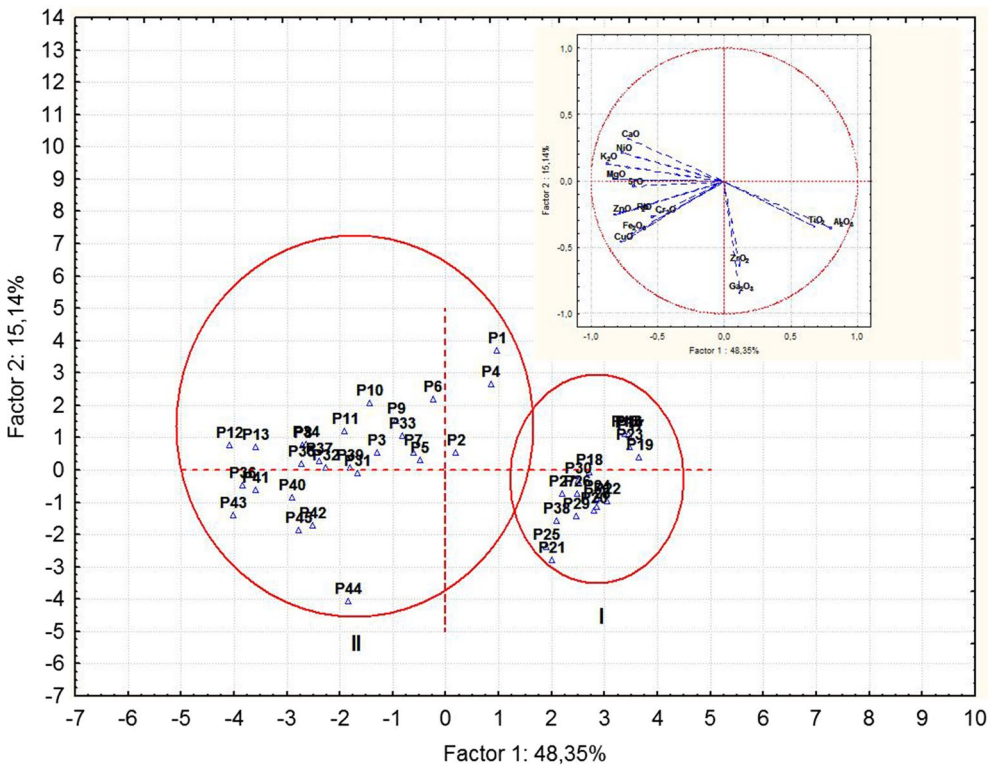

Fig. 6 Bi-plot of the first and second principal components—PCA performed on standardized oxide concentrations for Mg, Al, K, Ca, Ti, Cr, Fe, Ni, Cu, Zn, Ga, Rb, Sr and Zr—PIXE data for the ceramic paste

analyzed samples into two main compositional groups. A column in Table 1 also indicates to which of these two groups each sample belongs.

One of these groups (conventionally indicated with "I" in Fig. 6) is made out of 18 samples with relatively high Al_2O_3 (~ 24.9 mass% on average) and low CaO (~ 1.0 mass% on average) contents. This first group separates quite well from the rest of the other 27 ceramic fragments that cluster in a second group (marked with "II" in the same figure), regardless of their characteristics (decoration, granulation, firing etc.). This second group is characterized by relatively low Al_2O_3 (~ 17.7 mass% on average) and high CaO (~ 4.0 mass% on average) concentrations. As also visible from the loading plots shown in Fig. 6, the higher contents of Al are correlated with higher concentrations of Ti (group I), while the higher contents of Ca are correlated with higher concentrations of Mg, K and Sr (group II).

The first compositional group superposes relatively well with type I resulting from the petrographic analysis, except for sample P14 (containing 23.2 mass% Al_2O_3), attributed to type II from OM and sample P38 (with 24.6 mass% Al_2O_3) that belongs to type IV resulting from OM. Other discrepancy appears in the case of sample P42 (18.8 mass% Al_2O_3) that belongs to type I resulting from OM, and, at the same time, pertains to compositional cluster II, the one made out of the low-Al samples. Explanations for these discrepancies are still sought, but in any case, there seems to be a pattern that can be recognized from the analysis of the data obtained using these two different analytical techniques. Thus, paste I resulting from OM superposes quite well with the samples attributed to group I resulting from PCA; more or less, this reflects the use of a distinct type of clay that was chosen on purpose—most likely, to obtain vessels with different properties. On the other hand, the samples belonging to group II resulting from the PCA of PIXE data correspond to three types of paste (II, III and IV) revealed by OM. The most plausible explanation for this finding is that the shards belonging to these groups contain more or less the same minerals/compounds, hence the compositional similarity of the pellets (see also PIXE section). The differences between types II, III and IV of paste mainly consist in textural parameters, homogeneity and porosity, etc., and do not result from geochemistry.

A similar sub-division of potteries into two large groups, mainly separated by their Al and Ca contents, was also evidenced in the case of previously analyzed coeval ceramics from *Hârşova* and *Oltina* [7, 8].

Micro-PIXE scans of the interfaces between the decorated surfaces and the ceramic bodies were performed to identify the compound(s) responsible for the green glaze, as well as to estimate the thickness of these layers. A clear change in the chemical composition were observed for this type of decoration characterized by a large lead content (~ 64.4 mass% PbO on average, PbO content ranging from 50.4 to 76.8 mass%) compared to the ceramic body (~ 0.1 mass% PbO on average)—see Fig. 7 and Tables 3 and 4.

There are two ways of producing a Pb glazing: either by applying a Pb compound (e.g. litharge) as a suspension in water or by applying a mixture of PbO and quartz. In the former case, the glaze forms through direct reaction of PbO with the clay body; in the latter, the two components of the suspension react during firing, form a glaze that interacts with the body, and certain chemical elements (Al, Ca, Fe, Na, Mg) diffuse from the body into the glaze. These two glazing methods can be distinguished by subtracting the PbO content from the glaze composition and renormalizing the recipe to 100% and subsequently comparing this adjusted glaze composition with the one of the body [25–27]. Figure 8 shows that the Al_2O_3 content in the recast glaze composition is roughly the same as in the corresponding ceramic body, indicating that glazing was made through the application of lead oxide onto a non-calcareous ceramic body.

The micro-PIXE Pb Lα maps were used to estimate the thickness of the green glaze layer that turned out to range from 50 μm up to 300 μm. Some shards feature decorative layers with variable thickness.

Relatively small amounts of CuO (~ 1270 ppm on average) were found in the green glaze—see Table 4. The most likely explanation for the olive-green hues of the glaze is that they were induced by iron ions in reducing state [3, 4, 26, 28]. It must be mentioned here that certain amounts of Sb were determined in the composition of the green glaze covering samples P1 and P2—see Table 4. However, these particular two samples do not exhibit yellow hues, color that might have resulted from the presence of lead antimonate [3]; they are also olive-green, similar to the other five glazed samples analyzed in this study. The relatively small amounts of Sb from these two particular samples did not lead to any change in the appearance/coloring of their decorations. A possible explanation for the presence of Sb in the glaze is that this chemical element is a contaminant of the raw materials employed for making the glaze (in particular, of the lead compound).

The micro-PIXE scans of the interfaces did not provide any hint about what causes the shining of the golden engobe. However, the explanation was provided by OM: fine flakes of muscovite embedded in the slip produce the glittering golden shine of these shards. This decoration is the result of a different preparation manner and it did not imply the use of other raw materials.

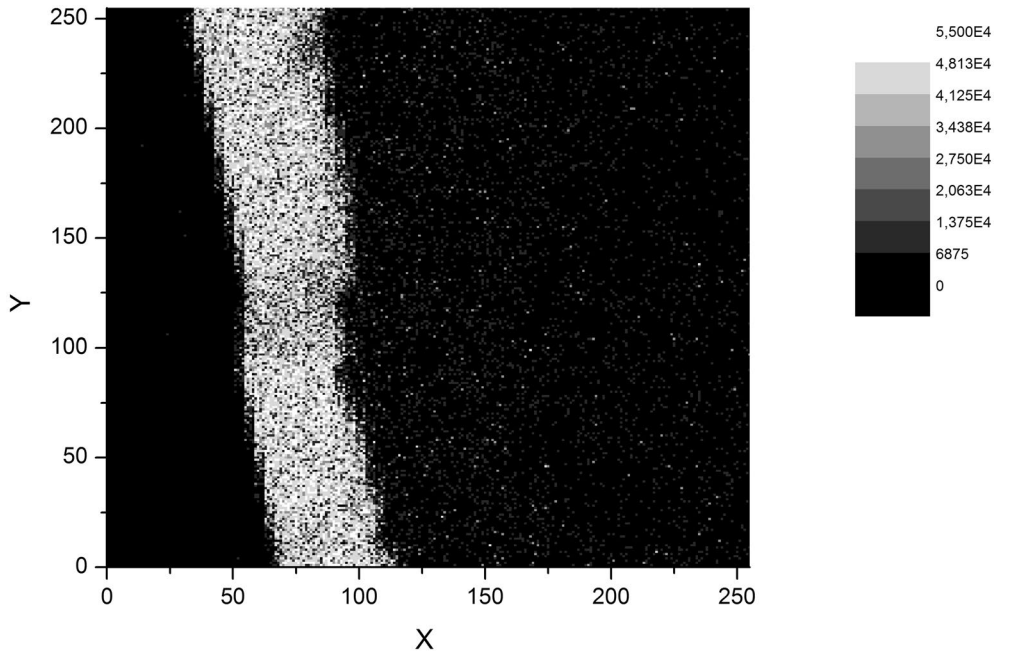

Fig. 7 Micro-PIXE Pb L_α map (750 × 750 μm^2) on glazed ceramic fragment no. 1—scan of a small area on the interface between the green glaze decoration and the underlying ceramic body

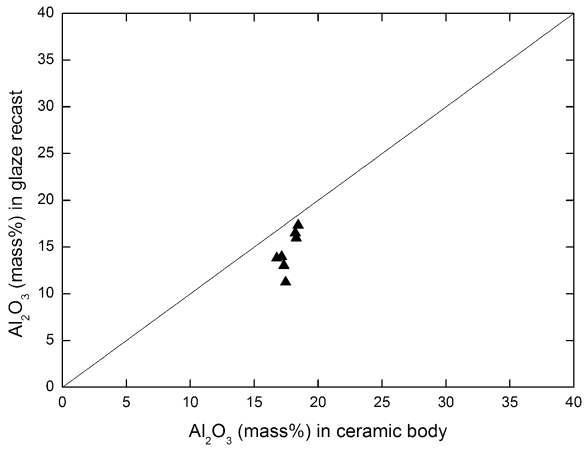

Fig. 8 Plot of the Al_2O_3 concentrations in the recast glaze composition and body composition—the points fall relatively close to the bisector, indicating that the glazing was made through the application of lead oxide onto the ceramic body

Discussions

From geological point of view, *Păcuiul lui Soare* area is characterized by the presence of Holocene clayey and sandy sediments, terrace deposits and Upper Pleistocene loessoid deposits [29].

Going south along the main valleys in the Southern Dobrudja area, beside consolidated rocks and the above-mentioned deposits, marly clays of Barremian age, sands and clays of Albian age, Ypresian clayey sands, quartz sands and clays of Tortonian age, greenish and brown clays and diatomites of Sarmatian age, gray and yellowish ferruginous sands, of the Dacian, and Levantine quartz sands with red sands intercalations can be encountered [29].

Summarizing, Southern Dobrudja region offers a wide range of raw materials that can be used for pottery making. The archaeometric analyses indicated that the Byzantine craftsmen from *Păcuiul lui Soare* chose in a natural way local sedimentary clays to produce ceramic vessels.

Kaolinitic clays were used in Dobrudja starting from the Roman period, as indicated by the discovery at Castelu of a kiln for pottery making and of some pits containing ceramic refuses [30]. Kaolinitic clays have been also employed during the Byzantine period from the ninth century AD onwards, but mostly during the tenth to eleventh centuries AD [31].

In Southern Dobrudja, important deposits of kaolinitic clays are known in the area of Medgidia, Cuza Vodă, Satu Nou, Țibrinu, and Tortoman, in the Carasu Valley, as well as on small tributaries, such as Agi Cabul and Adânca Valley. These deposits are in the form of lenticular layers separated by sand layers; this complex of Aptian age is situated above a layer of thick sands and below the Sarmatian lumachelic limestones [32]. These clays are formed by the kaolinisation of detrital feldspathic material in a

continental-lacustrine sedimentation environment. The color of the kaolinitic clay varies greatly from white to yellow, pink, and even bluish, depending on the amount and nature of the impurities (e.g. iron and manganese hydroxides) [32]. These deposits are situated on the Danube valley, the closest to *Păcuiul lui Soare* (approximately 50 km away) being the one nearby Cernavodă [33].

Other kaolinitic clay deposits are encountered as small outcrops in the form of lenses on Gîrlița valley, Oltina valley and southwest from Rasova, at distances between 12 and 35 km from *Păcuiul lui Soare* [29]. They contain small clay lenses, along with sands, pebbles and quartzitic micro-conglomerates, with intercalations of sands and limestone. However, the use of these deposits for pottery making during the Byzantine period remains to be demonstrated.

Byzantine kaolinitic clay vessels discovered in Dobrudja are characterized by an increased mechanical resistance—i.e. it is harder to break them compared to other potteries found at the same archaeological sites.

It seems that the potters from *Păcuiul lui Soare* knew about the kaolinitic clay deposits situated some tens of km from their settlement and they used this type of raw materials to make pots with good mechanical resistance. Thus, they could produce vessels not only different in appearance, as demonstrated by the different light hues of the paste, but mostly with better mechanical properties, hence justifying the effort of collecting some raw materials that were not readily available nearby their settlement.

Shards P1…P7 (the green glazed shards from the studied assemblage) and P8…P11 (the ones with golden engobe) belong to types II and III of paste resulting from OM analysis, i.e. potteries made from fine alluvial sediments. Compositionally, they belong to group II emerging from PCA. At this stage of research, we do not have any analytical argument to support the idea that these shards represent imported potteries, as they are similar in chemical compositional and mineralogy to the ceramic vessels that were locally produced from raw materials available nearby the settlement.

Conclusions

This paper describes the OM and micro-PIXE investigations on 45 ceramic shards dated to the eleventh century AD and in discovered in well-defined archaeological contexts at *Păcuiul lui Soare*, Romania, in a trial to identify the raw materials and working techniques employed for the manufacturing of these potteries, as well as to check some provenance hypotheses.

OM led to the identification of four types of pastes, similar to the ones evidenced for the coeval ceramics from *Hârșova* and *Oltina*, two archaeological sites located on the bank of the Danube River, relatively nearby *Păcuiul lui Soare.* PCA of the PIXE data singled out two compositionally distinct groups. The first one is made of the shards produced from Al-rich clays, possibly taken from a relatively nearby location from Dobrudja. The geology of the region and the archaeological discoveries indicated a possible source of kaolinitic clays located approximately 50 km north-east from *Păcuiul lui Soare*, source exploited starting with the Roman period. The second compositional group is composed of shards produced from several types of sedimentary raw materials that were locally available—most likely alluvial deposits of Danube and/or nearby lakes, as suggested by the petrographic data.

The Pb-rich green glaze was manufactured through the application of lead oxide onto a non-calcareous clay body, technology often encountered during the Roman and the Byzantine periods. The mica flakes present in the yellow engobe indicate that this type of decoration was produced by covering the vessels with a slip made of silty alluvial clay containing muscovite.

The results of this study demonstrated that the eleventh century AD pottery from *Păcuiul lui Soare*, with various appearances and playing different roles, was most likely locally manufactured using distinct raw materials, preparation and decoration techniques.

This research showed a marked similarity between the potteries from *Păcuiul lui Soare* and the ones excavated in the nearby Byzantine sites *Hârșova* and *Oltina*, indicating that during the eleventh century AD ceramic manufacturing in Dobrudja involved mostly the use of common local clays, but also of some pure, birefringent (possibly kaolinitic) clays from specific deposits, that were prepared using various recipes and techniques.

The archaeometric characterization performed using OM and PIXE did not provide any argument to suggest the presence of imported potteries among the analyzed ceramics from *Păcuiul lui Soare*.

The data reported in this paper contribute to the understanding of the way pottery was made during the eleventh century AD in the Lower Danube region, a topic little tackled until recently, and certainly of interest for the scholars involved in the study of the Byzantine period.

Acknowledgements

Leonardo La Torre is gratefully acknowledged for his skilled technical contribution in realizing the LNL experiment. The authors would like to express their gratitude to Dr. Oana Damian from Institutul de Arheologie "Vasile Pârvan", București, for providing the ceramic fragments discovered at *Păcuiul lui Soare* investigated in this study.

Authors' contributions

CT initiated this study and selected the archaeological material. CH realized the OM studies. RB and DC performed the PIXE analyses and interpreted the compositional data. All authors contributed to the discussions of the results. All authors read and approved the final manuscript.

Funding
This project has received funding from the European Union's Horizon 2020 research and innovation programme ENSAR2 under Grant agreement No. 654002.

Availability of data and materials
The datasets used and/or analysed during the current study are available from the corresponding author on reasonable request.

Competing interests
The authors declare that they have no competing interests.

Author details
[1] Horia Hulubei National Institute for Nuclear Physics and Engineering, 30 Reactorului Street, 077125 Măgurele, Romania. [2] Museum of National History and Archaeology, 900745 Constanța, Romania. [3] National Museum of Romania's History, 030026 Bucharest, Romania. [4] Dipartimento di Fisica e Astronomia "Galileo Galilei", Università di Padova, Padua 35131, Italy. [5] Istituto Nazionale di Fisica Nucleare (INFN) - Laboratori Nazionali di Legnaro (LNL), Legnaro 35020, Italy.

Received: 22 January 2019 Accepted: 19 July 2019
Published online: 30 July 2019

References

1. Charalambous AC, Sakalis AJ, Kantiranis NA, Papadopoulou LC, Tsirliganis NC, Stratis JA. Cypriot Byzantine glazed pottery: a study of the Paphos workshops. Archaeometry. 2010;52:628–43.
2. Damjanović L, Bikić V, Šarić K, Erić S, Holclajtner-Antunović I. Characterization of the early Byzantine pottery from Caričin Grad (South Serbia) in terms of composition and firing temperature. J Arch Sci. 2014;46:156–72.
3. Kirmizi B, Göktürk EH, Colomban Ph. Colouring agents in the pottery glazes of Western Anatolia: new evidence for the use of *Naples yellow* pigment variations during the Late Byzantine period. Archaeometry. 2015;57:476–96.
4. Lyubomirova V, Šmit Ž, Fajfar H, Kuleff I. Determination of the chemical composition of medieval glazed pottery from Drastar (Bulgaria) using PIXE/PIGE and LA-ICP-MS. Composition chimique de poterie glaçurée médiévale de Drastar (Bulgarie) déterminée par PIXE-PIGE et LA-ICP-MS. ArchéoSciences/J Archaeom. 2017;41:69–82.
5. Palamara E, Zacharias N, Xanthopoulou M, Kasztovszky ZS, Kovács I, Palles D, Kamitsos EI. Technology issues of Byzantine glazed pottery from Corinth, Greece. Microchem J. 2016;129:137–50.
6. Waksman SY, Skartsis SS, Kontogiannis ND, Todorova EP, Vaxevanis G. Investigating the origins of two main types of middle and late Byzantine amphorae. J Archaeol Sci Rep. 2018;21:1111–21.
7. Bugoi R, Talmațchi C, Haită C, Ceccato D. Archaeometric studies of Byzantine pottery from Hârșova–Carsium, Romania. Nucl Instrum Methods B. 2015;348:296–301.
8. Bugoi R, Talmațchi C, Haită C, Ceccato D. Characterization of Byzantine pottery from Oltina (Constanța County), Romania, using PIXE and optical microscopy. Nucl Instrum Methods B. 2018;417:110–4.
9. Burghelea V, Stoian I, Mănucu-Adameşteanu Gh, Poll I, Pasuk I. Byzantine ceramic from XI–XIIth centuries at Piatra-Frecăței archaeological site (Tulcea County). Key Eng Mat. 2004;264–268:2379–82.
10. Baraschi S. Ceramica cu angobă aurie (secolele XI–XII). Studii și Cercetări de Istorie Veche și Arheologie. 1989;40:187–98.
11. Barnea I. Amforele feudale de la Dinogetia. Studii și Cercetări de Istorie Veche. 1954;5:513–28.
12. Barnea I. Ceramica de import. In: Ștefan GH, Barnea I, Comșa M, Comșa E, editors. Dinogeia. I. Așezarea feudală timpurie de la Bisericuța-Garvăn. București: Editura Academiei RSR; 1967. p. 229–76.
13. Paraschiv-Talmațchi C, Custurea G. Nouvelles données sur les découvertes sous-aquatiques du littoral roumain. Pontica. 2015–2016;48–49:241–79.
14. Diaconu P, Vîlceanu D. Păcuiul lui Soare. Cetatea bizantină. I, București: Editura Academiei RSR; 1972. p. 23–5, 89.
15. Diaconu P. Rolul cetății din insula Păcuiul lui Soare în cadrul situației politice a Dobrogei la sfârșitul secolului X. Pontica. 1969;2:395–400.
16. Diaconu P, Baraschi S. Păcuiul lui Soare. Așezarea medievală (secolele XIII–XV). II. București: Editura Academiei RSR; 1977. p. 7–9.
17. Baraschi S. Un cuptor de ars oale de la Păcuiul lui Soare (secolul al XI-lea). Studii și Cercetări de Istorie Veche și Arheologie. 1974;25:461–71.
18. Baraschi S. O ștampilă de bronz de la Păcuiul lui Soare. Studii și Cercetări de Istorie Veche. 1973;24:541–4.
19. Waksman Y, Girgin Ç. Les vestiges de production de céramiques des fouilles de Sirkeci (Istanbul). Premiers éléments de caractérisation. Anatolia Antiqua. 2008;16:443–69.
20. Courty MA, Goldberg P, Macphail R. Soils and micromorphology in archaeology. Cambridge: Cambridge University Press; 1989. p. 63–75.
21. Haită C. Observations at microscope on pottery fabric of some ceramic fragments from Gumelnița *tell* settlements Hârșova and Borduşani. Studii de Preistorie. 2012;9:113–21.
22. Quinn PS. Ceramic petrography. The interpretation of archaeological pottery and related artefacts in thin section. Oxford: Archaeopress; 2013. p. 71–103.
23. Boccaccio P, Bollini D, Ceccato D, Egeni GP, Rossi P, Rudello V, Viviani M. The LNL proton microprobe: original technical solutions and new developments. Nucl Instrum Methods B. 1996;109–110:94–8.
24. Campbell JL, Boyd NI, Grassi N, Bonnick P, Maxwell JA. The Guelph PIXE software package IV. Nucl Instrum Methods B. 2010;268:3356–63.
25. Tite MS, Freestone I, Mason R, Molera J, Vendrell-Saz M, Wood N. Lead glazes in Antiquity-methods of production and reasons for use. Archaeometry. 1998;40:241–60.
26. Walton MS, Tite MS. Production technology of Roman lead-glazed pottery and its continuance in Late Antiquity. Archaeometry. 2010;2010(52):733–59.
27. Waksman SY, Bouquillon A, Cantin N, Katona I. Approche archéométrique des premières "Byzantine glazed white ware" et de productions glaçurées romaines et romaines tardives. Rei Cretariae Romanae Acta. 2008;40:531–6.
28. De Vito C, Medeghini L, Garruto S, Coletti F, De Luca I, Mignardia S. Medieval glazed ceramic from Caesar's Forum (Rome, Italy): production technology. Ceram Int. 2018;44:5055–62.
29. Bandrabur T, Patrulius D. Harta geologică a R.S.R., scara 1:200.000, Foaia 45 Călărași. Notă explicativă, București: Institutul Geologic, Comitetul de Stat al Geologiei; 1967.
30. Băjenaru C. The Late Roman kaolinic pottery produced in the province of Scythia. In: Rusu-Bolindeț V, Roman CA, Gui M, Iliescu IA, Botiș FO, Mustață S, Petruț D, editors. Atlas of Roman pottery workshops from the provinces Dacia and Lower Moesia/Scythia Minor (1st–7th centuries AD) (I). Cluj-Napoca: Mega Publishing House; 2018. p. 239–57.
31. Comșa M. Cu privire la evoluția culturii balcano-dunărene în sec. IX–XI (Studiu preliminar). Studii și Cercetări de Istorie Veche. 1963;14:107–22.
32. Brana V, Avramescu C, Călugăru I. Substanțe minerale nemetalifere. Bucureşti: Editura Tehnică; 1980. p. 111–2.
33. Chiriac M, Mutihac V, Mirăuță O, Mînzatu S. Harta geologică a R.S.R., scara 1:200.000, Foaia 46. Constanța: Institutul Geologic, Comitetul de Stat al Geologiei; 1968.

Publisher's Note